

A Parallel Graded-Mesh FDTD Algorithm for Human–Antenna Interaction Problems

Luca Catarinucci
Luciano Tarricone

Innovation Engineering Department, University of Salento, Lecce, Italy

The finite difference time domain method (FDTD) is frequently used for the numerical solution of a wide variety of electromagnetic (EM) problems and, among them, those concerning human exposure to EM fields. In many practical cases related to the assessment of occupational EM exposure, large simulation domains are modeled and high space resolution adopted, so that strong memory and central processing unit power requirements have to be satisfied. To better afford the computational effort, the use of parallel computing is a winning approach; alternatively, subgridding techniques are often implemented. However, the simultaneous use of subgridding schemes and parallel algorithms is very new. In this paper, an easy-to-implement and highly-efficient parallel graded-mesh (GM) FDTD scheme is proposed and applied to human–antenna interaction problems, demonstrating its appropriateness in dealing with complex occupational tasks and showing its capability to guarantee the advantages of a traditional subgridding technique without affecting the parallel FDTD performance.

numerical dosimetry FDTD graded mesh human–antenna exposure parallel computing

1. INTRODUCTION

In recent years, an extraordinary and continuous growth of the communication technologies has been observed, with the consequent capillary diffusion of many electromagnetic (EM) sources on the territory, e.g., radio-base station antennas (RBAs), mobile hand-phones, wi-fi access points, which cause the frequent interaction between humans and EM fields. As a direct consequence, the joint interest of public opinion and scientific community in the possible human-health hazards caused by exposure to EM sources has become relevant with the consequent strong necessity to rigorously evaluate the EM impact in occupational EM exposure. To evaluate such hazards the energy absorbed by human tissues exposed to EM radiation must be evaluated: to this aim, both numerical and experimental approaches are used.

Several issues of the problem, such as the shape of the human body, tissue characteristics, the

geometry of EM sources, need to be modeled with adequate accuracy. For instance, experimental approaches based on simplified models of the human body cannot be adopted because they introduce large approximation errors. Fortunately many accurate numerical human body models (numerical phantoms) are available in the literature, such as the ones proposed in Zubal, Harrell, Smith, et al. [1] and Mason, Ziriak, Hurt, et al. [2]. Furthermore many EM numerical solvers can be used, the finite difference time domain (FDTD) [3] method being a rather attractive candidate.

Through FDTD, in fact, both the antennas and the human phantoms can be accurately modeled by choosing a relatively fine mesh, thus giving a rigorous full-wave solution. Parallel computing, offering both large memorization space and huge computing power, seems to be the best way to solve such a challenging problem [4, 5].

In such a context, the necessity to describe complex structures (such as EM sources and

human bodies) imposes a fine discretization step; if a uniform mesh is adopted, the waste of computational resources can become excessive. Furthermore, by implementing traditional subgridding techniques [6, 7], consisting in the use of a fine mesh only in selected specific areas, the number of computational grid points can be appreciably reduced. However, the structure of a standard FDTD algorithm will vary strongly, because of the need of a proper interpolation/extrapolation process in the fine-mesh/coarse-mesh interfaces. Consequently, the algorithm parallelization becomes not trivial and the performance perspective not encouraging. Nevertheless, by renouncing some of the advantages of the traditional subgridding schemes, a good compromise among memory saving capability, implementation simplicity (also on parallel platforms) and performance, can be reached by the proposed graded-mesh (GM) technique.

2. FDTD METHOD

The FDTD method, firstly proposed by Yee in 1966 [3], is nowadays one of the most used approaches to solve Maxwell's partial differential equations, because of its high versatility. Extensive literature is available about this topic, so we will just briefly mention here that the FDTD algorithm is based on temporal and three-dimensional spatial discretization and it transforms the time-dependent Maxwell's curl equations into a set of finite-difference relations [3, 8, 9]. Also, on the edge of the simulation domain, boundary conditions are needed; among the several possible choices [9, 10, 11, 12], Mur's absorbing boundary conditions (ABC) are used. In fact, even though perfect matched layer (PML) ABCs can be more accurate, they are more time-consuming, and their implementation on parallel architectures such as the one here adopted is not trivial at all. Anyway, Mur's ABCs guarantee accuracy appropriate for the problem, as it is demonstrated in the following sections.

3. PARALLEL FDTD

In this section the basic idea behind the parallel implementation of the FDTD algorithm is shortly given. On a machine with n processors, the whole computation domain is divided into n subdomains (with equal volume and shape). In particular, the domain is divided along the x dimension, mapping in each processor a subregion D'_i of size $[\frac{N_x}{n} \times N_y \times N_z]$; for the sake of simplicity we suppose N_x to be an integer multiple of n . The EM field components are updated in each processor in the same instant. When the computation updates a field component on the border of the domain, some values belonging to the border of the adjacent domain are required: to avoid communications during the computations, each subdomain is surrounded by the border cells of the other domain. These border values are communicated after the updating phase. See Catarinucci, Palazzari and Tarricone for more details and for the scheme of the FDTD parallel algorithm [4].

4. PARALLEL GRADED-MESH (GM) FDTD

When using uniform FDTD meshing, the characterization of simulated objects with an adequate spatial resolution forces the adoption of such a resolution over the entire simulation domain. Nevertheless, a larger spatial discretization step could be applied wherever spatial accuracy is not needed. Such an observation is the basis of GM FDTD algorithms which, allowing the existence of different discretization steps in different regions, give a certain level of accuracy for the solution using less memory and computational power than the ones needed to obtain the same accuracy with a classic (uniform) FDTD scheme.

Many authors have already adopted FDTD computation schemes with nonuniform step with interesting results when traditional computer are adopted [6, 7]. To the best of our knowledge, instead, the use of variable step gridding techniques within a parallel computing

scheme is substantially new in literature. This is probably because the aforementioned subgridding techniques perform the evaluation of the EM field components through additional extrapolation and interpolation operations, strongly varying the FDTD scheme, making parallelization not trivial and decreasing the performance.

Differently, this paper introduces a GM scheme (GM-FDTD) which is a natural extension for a parallel FDTD implementation. In GM-FDTD the discretization is performed in a way so that each grid cell has only one adjacent grid cell for each

of its six faces. Furthermore, along each direction the space step can be arbitrarily varied, within the limits imposed by the stability criterion, allowing very smooth transitions between a fine and a coarse mesh region. Taking previous advantages into consideration, a price in terms of memory has to be paid: to guarantee such properties, in fact, the fine-mesh regions cannot be strictly limited only to the interested region, but must be extended up to the limit of the simulation domain. Figure 1 shows such differences.

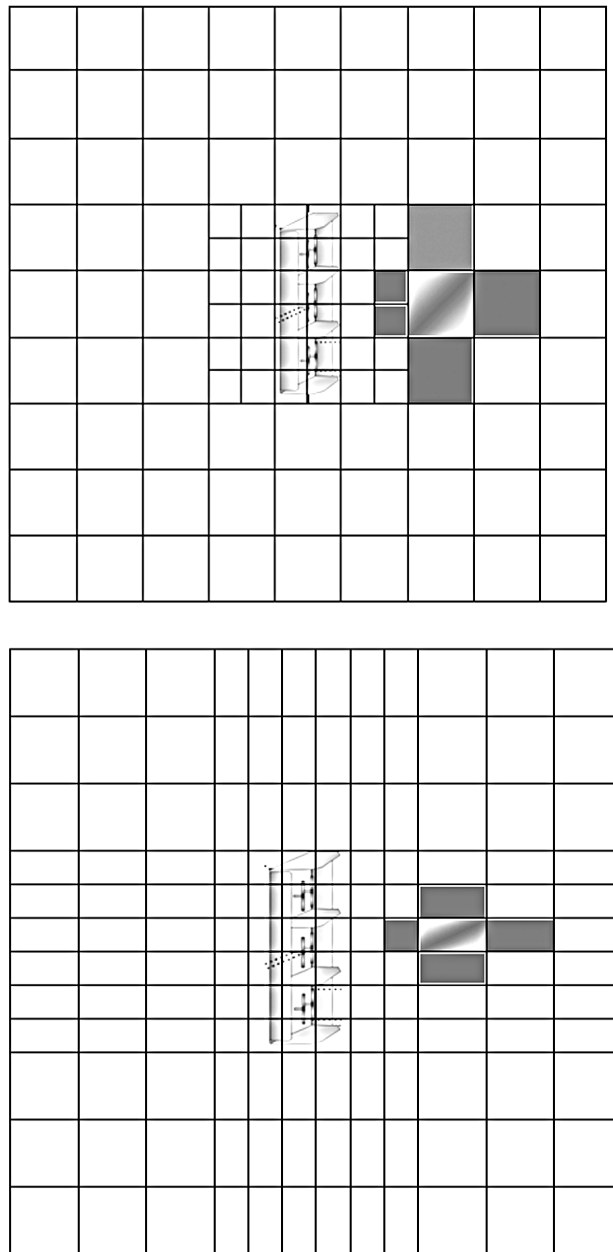


Figure 1. Modeling of an electromagnetic source by standard subgridding techniques (top) and by the proposed graded-mesh technique (bottom).

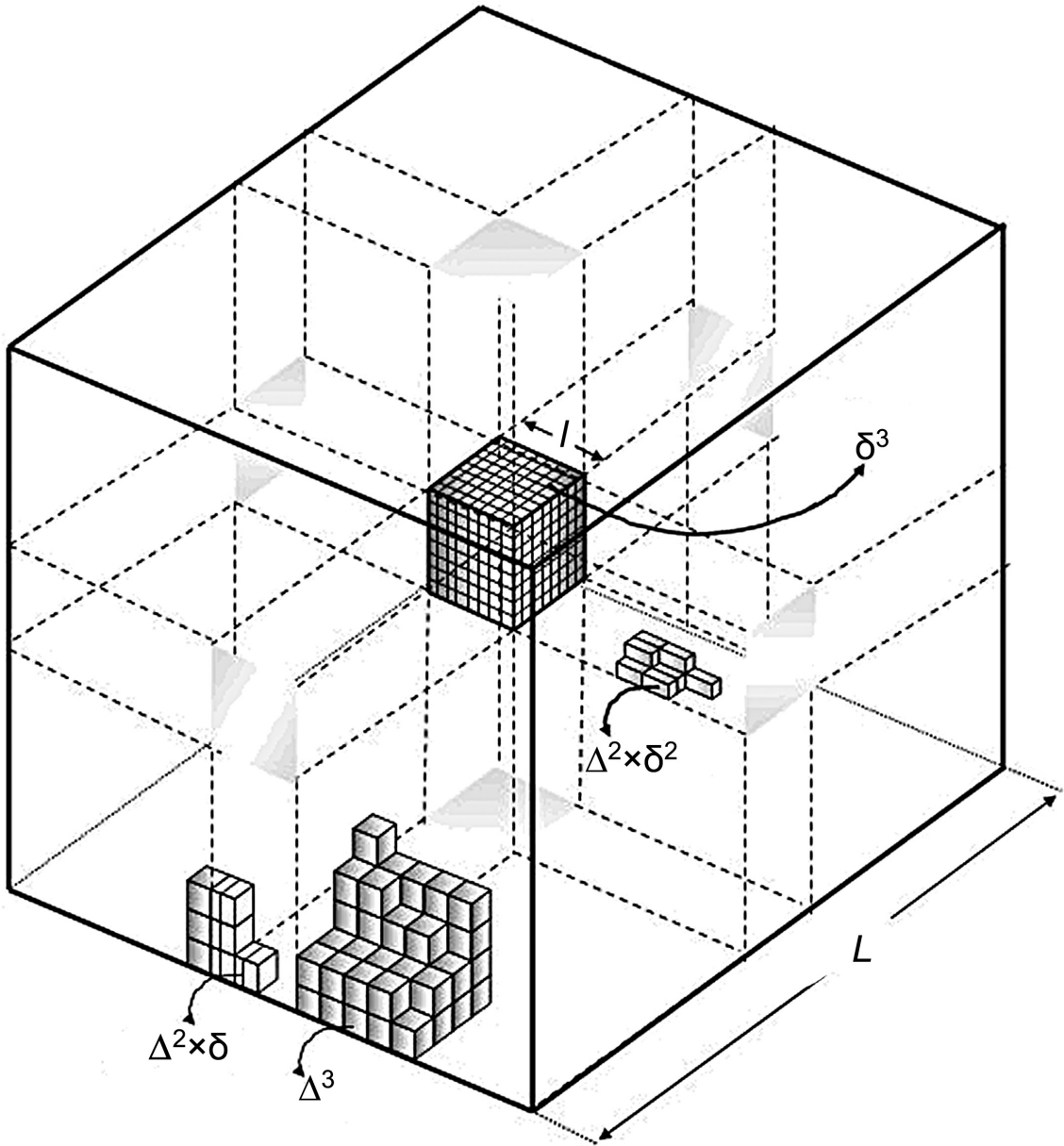


Figure 2. A three-dimensional mesh example for the variable-mesh finite difference time domain method. Notes. L, l —linear dimensions, Δ, δ —steps.

To quantify the cost of the simulation, in terms of used domain cells, let us refer to Figure 2 and consider the simple case of a cubed domain, having linear dimension L , with an object inscribed in a cube of size l . The object should be discretized at step δ , while the whole domain can be discretized with step Δ . The simulation, if carried on at the smallest discretization step, would require a number of grid cells

$$N_{\text{cells}}(\delta) = (L/\delta)^3. \quad (1)$$

Neglecting the eventual transition layer between regions with different discretization steps, conventional subgridding techniques would require a number of grid cells

$$N_{\text{cells}}(\Delta, \delta) = (L/\Delta)^3 - (l/\Delta)^3 + (l/\delta)^3. \quad (2)$$

Referring to Figure 2, it is easy to verify that the GM-FDTD method would require a number of grid cells

$$N_{\text{cells}}(\text{GM-FDTD}) = ((L-l)/\Delta)^3 + (l/\delta)^3 + 3 \cdot [(L-l) \cdot l^2 / (\Delta \delta^2)] + 3 \cdot [l \cdot (L-l)^2 / (\Delta^2 \delta)]. \quad (3)$$

For the sake of simplicity, in previous expressions we assumed Δ to be an exact divisor of L , l and $(L - l)$ and δ to be an exact divisor of L and l .

Both computational and memory requirements of the FDTD method increase linearly—according to a first-order approximation—with the number of grid cells. Therefore we define the performance gain (PG) of the GM scheme with respect to the standard, fine meshing (FM), as

$$PG(GM) = \frac{N_{\text{cells}}(FM) - N_{\text{cells}}(GM)}{N_{\text{cells}}(FM)}. \quad (4)$$

In a similar way, the PG between two different GM schemes, GM_1 and GM_2 is given by

$$PG(GM_1, GM_2) = \frac{PG(GM_1) - PG(GM_2)}{PG(GM_1)}. \quad (5)$$

For the described case of a small cube (linear size l , discretized with step δ) inscribed in a larger cube (linear size L , discretized with step Δ), the PG of conventional subgridding techniques (CS) with respect to the uniform meshing with step δ is

$$PG(CS) = \frac{\Delta^3 - \delta^3}{\Delta^3} \cdot \frac{L^3 - l^3}{L^3} \quad (6)$$

for the same case, the PG of the GM-FDTD method with respect to the uniform meshing with step δ is

$$PG(GM - FDTD) = \frac{(L/\delta)^3 - N_{\text{cells}}(GM - FDTD)}{(L/\delta)^3}. \quad (7)$$

For instance, if we fix $L = 2$ m, $l = 0.1$ m, $\Delta = 0.01$ m and $\delta = 0.002$ m, the PG of CS is $PG(CS) = 0.992$, while $PG(GM-FDTD) = 0.986$; in spite of a small decrease in performances ($\sim 0.6\%$), the GM-FDTD method allows an easier, and more efficient, parallel implementation and shows a better numerical behavior, avoiding interpolation/extrapolation procedures and allowing smooth transitions between regions with different discretization steps.

The parallel implementation is based on the same principles of the parallel uniform FDTD, i.e., it adopts the same partition of the simulation domain, based on a balance of the computation among the different processors, and implements

the same communication pattern between adjacent processors.

To take into account the different cell-size, three auxiliary vectors can be used, containing the dimension of each cell along x , y and z . Now, because of the component location in Yee's cell [8], such values can be directly used wherever E-field space derivatives are evaluated; instead, when H-field space derivatives are considered, the averaged dimension between two adjacent cells must be used. The same kind of arrangement must be applied in the ABC computation too.

5. RESULTS

To verify performance and accuracy of parallel GM-FDTD, we tested it on some real cases. First, we considered the simulation of many different kinds of real 900 MHz RBAs and we evaluated an electric field pattern at a fixed near-field distance (here called near-field radiation pattern, NFRP) from the antenna.

After a cubical mesh for the source discretization had been chosen, the uniform (U) NFRP obtained by using the same space-step everywhere was evaluated and compared with NFRPs at the same physical distance but using different GM schemes. The comparison among such patterns is a relevant test: it has to be observed in fact that, differently from standard radiation patterns, which are evaluated in the far field region and are expressed in decibels, NFRPs are strongly dependent on the observation distance, the values being expressed in volts per meter with the evaluation performed at a generic source-distance. Figure 3, e.g., shows the vertical plane U-NFRP using a cubical mesh of $6 \times 6 \times 6$ mm³ and a GM-NFRP where space step varies from 6 mm in the source region, to 18 mm elsewhere (according with the previously discussed GM rules). The really good agreement between them is quite evident.

To quantify differences among various NFRPs as well as to investigate the effects of the variability of the mesh on the accuracy, in the GM scheme cases direct transitions to 12, 18 and 24 mm have been realized. Furthermore the cases of four smoother transitions from 6 to

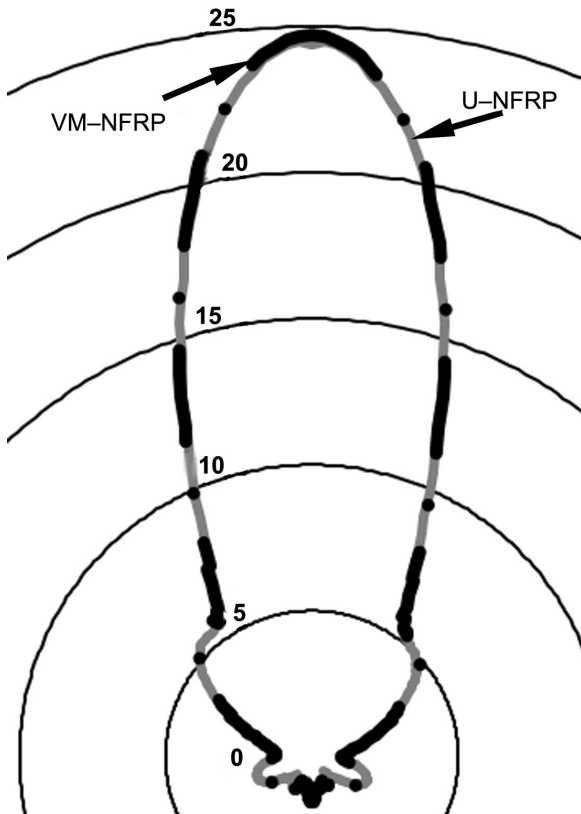


Figure 3. Uniform near-field radiation pattern (U-NFRP) versus 6–18 mm graded-mesh near-field radiation pattern (GM-NFRP).

12 mm, using a certain number of 9-mm cells in between, have been considered. For each case, the averaged errors with respect to the reference U-NFRP have been reported in Table 1. Despite a strong step-size variation, differences smaller than 2% are obtained. For the four studied 6–9–12 meshes, an error reduction is observed by varying the size of the transaction region.

TABLE 1. Uniform Versus Graded Mesh

Kind of Mesh	Error (%)
6–12	2.01
6–9–12 (10 cells)	1.70
6–9–12 (20 cells)	1.31
6–9–12 (30 cells)	1.31
6–9–12 (40 cells)	1.32
6–18	1.97
6–24	2.36

Results in Table 2 refer to the speed-up on a 12-processor parallel computer (SGI Altix 350; SGI, USA) by varying the dimension of the simulation domain. They refer to one particular case of a GM scheme where almost half of the used cells have 6-mm steps, whilst 12-mm ones are used elsewhere. However, the same speed-ups have been obtained for every chosen mesh, the computational time for this algorithm being dependent only on the minimum space step. Hence, differently from other kinds of subgridding techniques, performance is not affected by the chosen mesh. Moreover, in Table 2 a super-linear behavior is apparent in some cases; it depends on the well-known cache effects.

TABLE 2. Achieved Graded-Mesh Finite Difference Time Domain Speed-Up on an SGI Altix 350 (SGI, USA) Architecture

Domain	num_proc				
	1	2	4	8	12
100 × 100 × 100	1	1.93	3.82	8.66	12.17
200 × 200 × 200	1	1.91	3.73	7.91	11.21
250 × 250 × 250	1	1.93	3.81	7.29	11.02

Finally, Figures 4–5 report the electric field levels for the occupational problem of a worker's exposure to the field emitted by RBAs, showing the appropriateness of such a method to deal with large EM problems. In both cases, a domain of $256 \times 256 \times 256$ cells has been modeled, using a uniform mesh with 4-mm steps for the simulation of Figure 4, and a GM scheme with 4-mm steps in the source region and in the body region and 12-mm ones elsewhere for the case of Figure 5.

The advantage in terms of maximum reachable human–antenna distance is apparent: referring to the case of Figure 5, the same human–antenna distance using a cubical uniform mesh, could be studied by modeling a domain of almost $450 \times 450 \times 450$ cells, with a memory requirement and a computational time which would be 5 times higher.

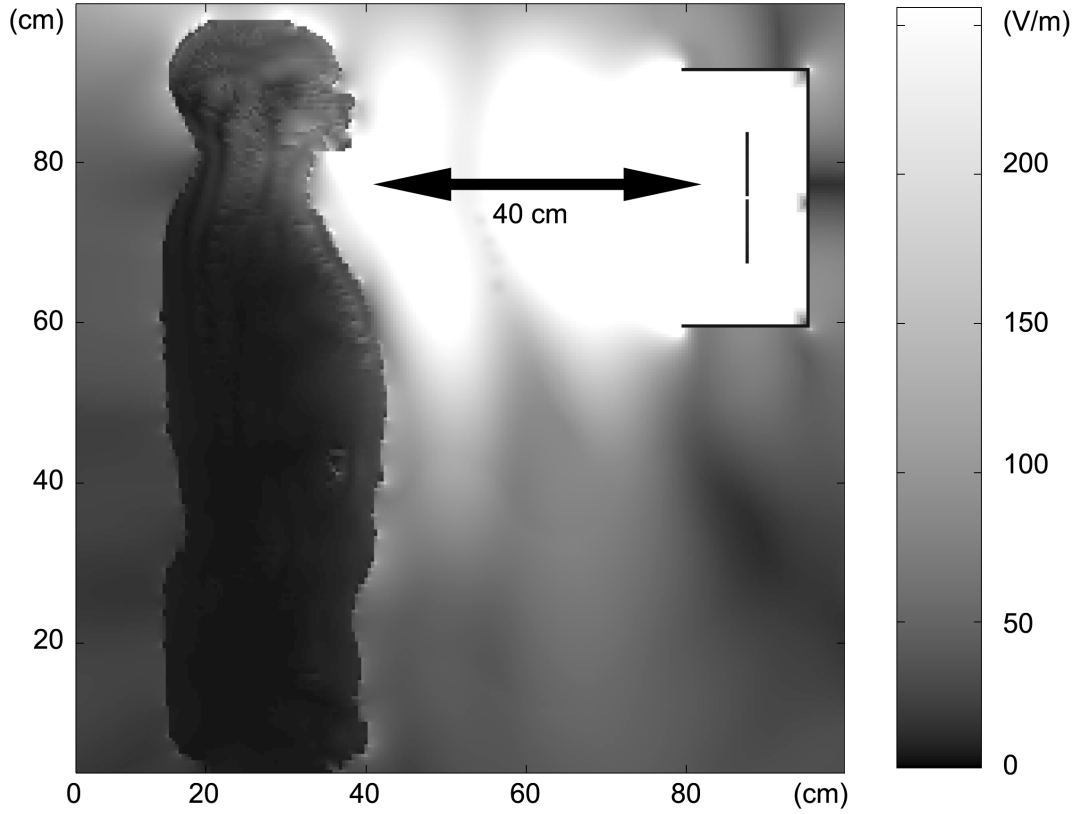


Figure 4. Human-antenna interaction problem by using a 4 mm^3 uniform mesh. The electric field level is shown by considering a radiated power of 32 W and a working frequency of 900 MHz.

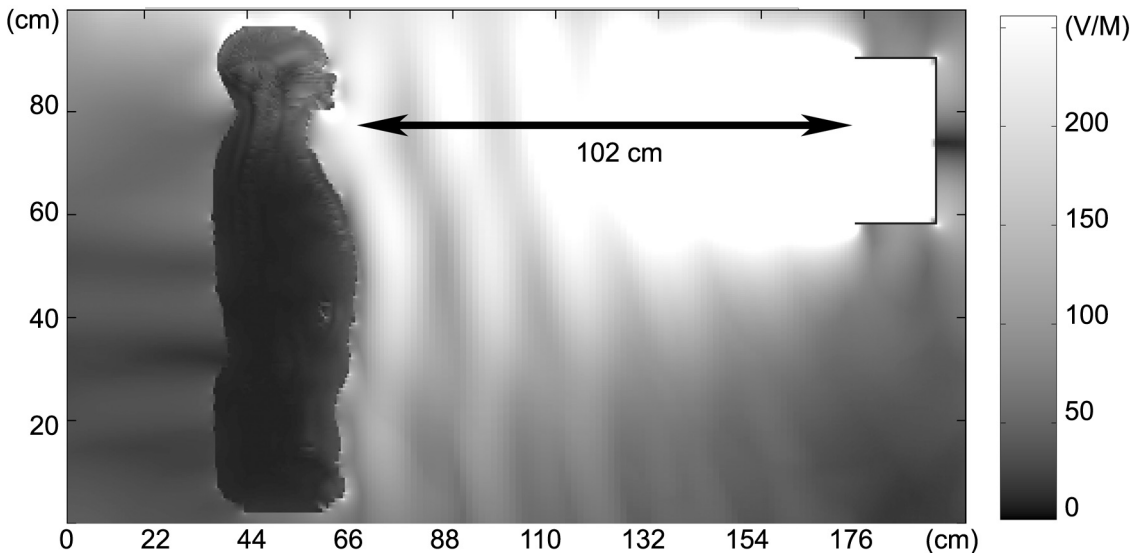


Figure 5. Human-antenna interaction problem by using a 4-12 mm graded-mesh scheme. The shown electric field level has been computed in the same working condition as Figure 4.

6. CONCLUSIONS

We presented the parallel implementation of an algorithm devoted to the simulation of large EM problems which is particularly useful for assessing occupational exposures to EM fields. In such an area, a realistic simulation domain including at least antennas and human phantoms, should be accurately modeled. The possible scenarios (different human postures, large antennas, complicated environment, etc.) can result in very complex and large simulation domains, difficult to be studied with standard algorithms and traditional numerical platforms if an adequate accuracy is required. The proposed algorithm is based on the FDTD method including a GM feature. After a brief review of the FDTD algorithm, we described its parallel implementation, and discussed the proposed GM peculiarities. The relevant topic of the interaction between RBAs and humans has been studied and the advantages in terms of memory-saving have been estimated, demonstrating the appropriateness of the proposed tool to deal with difficult EM problems.

REFERENCES

1. Zubal C, Harrell CR, Smith EO, Rattner Z, Gindi G, Hoffer PB. Computerized 3D segmented human anatomy. *Med Phys.* 1994;21(2):299–302.
2. Mason PA, Ziriak JM, Hurt WD, Walters TJ, Ryan KL, Nelson DA, et al. Recent advancements in dosimetry measurements and modeling. In: Klauenberg BJ, Miklavcic D, editors. *Radio frequency radiation dosimetry*. Norwell, MA, USA: Kluwer; 2000. p. 141–55.
3. Yee KS. Numerical solution of initial boundary value problems involving Maxwell's equations in isotropic media. *IEEE Trans Antennas Propag.* 1966;AP-14(4):302–7.
4. Catarinucci L, Palazzari P, Tarricone L. Human exposure to the near field of radiobase antennas: a full-wave solution using parallel FDTD. *IEEE Trans Microw Theory Tech.* 2003;51:935–40.
5. Guiffaut C, Mahdjoubi K. A parallel FDTD algorithm using the MPI library. *IEEE Antennas Propagat Mag.* 2001;43(2):94–103.
6. Yu W, Mittra R. A new higher-order subgridding method for finite difference time domain (FDTD) algorithm. *IEEE Ant and Prop Society Int Symp.* 1998;1:608–11.
7. Okoniewski M, E. Okoniewska E, Stuchly MA. Three-dimensional subgridding algorithm for FDTD. *IEEE Trans Antennas Propag.* 1997;45:422–9.
8. Taflove A, Brodwin ME. Numerical solution of steady-state electromagnetic scattering problems using the time-dependent Maxwell's equations. *IEEE Trans Microw Theory Tech.* 1975;MTT-23(8):623–30.
9. Taflove A. *Computational electrodynamics, the finite difference time-domain method*. Norwood, MA, USA: Artech House; 1995.
10. Mur G. Absorbing boundary conditions for the finite-difference approximation of the time-domain electromagnetic-field equations. *IEEE Trans Electromagn Compat.* 1981;EMC-23(4):377–82.
11. Berenger JP. A perfectly matched layer for the absorption of electromagnetic waves. *J Comput Phys.* 1984;114:185–200.
12. Berenger JP. Perfectly matched layer for the FDTD solution of wave-structure interaction problems. *IEEE Trans Microw Theory Tech.* 1996;44:110–7.